Inorganic Chemistry

Open Access
This article is licensed under CC-BY 4.0

pubs.acs.org/IC
Article

La−Ni−Si: A Gold Mine with a Diamond

Volodymyr Smetana, Davide Grilli, Vitalii Shtender, Marcella Pani,* Pietro Manfrinetti,* and Anja-Verena Mudring*

Cite This: *Inorg. Chem.* 2024, 63, 22761−22770

Read Online
ACCESS | Metrics & More | Article Recommendations | Supporting Information

ABSTRACT: The La-poor part of the ternary La−Ni−Si system has been explored leading to the discovery and structural characterization of four new polar intermetallic compounds. $LaNi_5Si_2$ [$BaAu_5Ga_2$ type, *oP*64, space group *Pnma*, a = 7.8223(7) Å, b = 6.3894(6) Å, c = 17.843(2) Å, V = 891.8(2) Å^3, Z = 8] features a diamond (lonsdaleite)-like homoatomic Ni framework and is the first Ni representative of a larger family of compounds typically formed by aurides. $La_2Ni_8Si_3$ [$Eu_2Ni_8Si_3$ type, *tP*52, $P4_2/nmc$, a = 10.0278(3) Å, c = 7.5047(4) Å, V = 754.65(6) Å^3, Z = 4] is characterized by homoatomic Ni_4 tetrahedra and rectangles. $LaNi_5Si_3$ [$SrNi_5P_3$ type, *oS*36, *Cmcm*, a = 3.722(2) Å, b = 11.759(5) Å, c = 11.622(3) Å, V = 508.7(3) Å^3, Z = 4] is governed by extensive heteroatomic bonding and characterized by homopolyhedral packing. $La_3Ni_4Si_2$ [$Ce_3Ni_4Si_2$ type, *mC*36, *C*2/*c*, a = 15.819(1) Å, b = 6.0068(5) Å, c = 7.4918(6) Å, β = 103.163(5)°, V = 693.17(10) Å^3, Z = 4] is a new member of homologous series that includes $La_3Ni_3Si_2$ and $La_3Ni_{3.5}Si_2$. We conclude that the similar radii and electronegativities of Ni and Si are the reason for the incredible diversity of compositions and structures in this system.

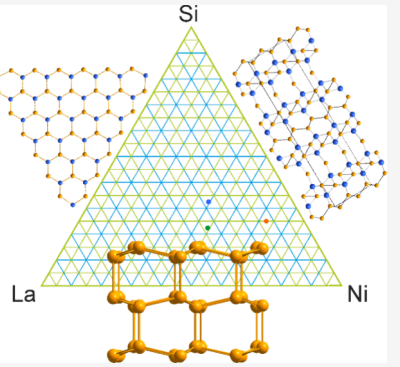

Downloaded via UNIV DEGLI STUDI DI GENOVA on December 6, 2024 at 14:48:55 (UTC).
See https://pubs.acs.org/sharingguidelines for options on how to legitimately share published articles.

INTRODUCTION

Although formally not a metal, silicon exhibits a crystal chemistry that is frequently identical or very close to pure intermetallics.[1,2] Metal silicides occur for a vast abundance of compositions and feature a large variety of structural motifs.[3] Therefore, intermetallic silicides form a class of compounds that links true intermetallics and ionic compounds. This is also reflected in the materials properties and silicides have found broad applications in high-temperature coatings,[4,5] microelectronics,[6,7] catalysis,[8] etc. Ternary silicides, particularly those with rare-earth and/or transition metals are famous for their giant magnetocaloric effect,[9,10] superconductivity[11,12] or hydrogen sorption properties.[13]

As Si is, on the one hand, close in size[14] and electronegativity[15] to other metalloids as well as some nonmetals, and on the other, late 3*d* metals, a wide range of compositions can be realized is such systems, which gives plenty of possibilities for property tuning. Being a very abundant element in nature, silicon allows for production scaling circumventing any supply interruptions. A particularly rich chemistry can be observed for ternary silicides with transition metals and lanthanides.[3] The respective ternary systems frequently feature good miscibility and, consequently, good variability of compositions and high structural diversity.

The La−Ni−Si system recently attracted our attention due to the enormous richness of the reported compositions with all the new findings being stunningly detected in compositionally small narrow regions frequently forming closely related series.[16−18] Efforts to investigate the phase equilibria in this system in detail point to an even larger number of hidden islands of compounds. Interestingly, a preprint on phase equilibria at 1070 K[19] misses all these recent findings, while phase equilibria reported at 673 K[20] are limited to just 14 ternary compounds. Although some phases may undergo an eutectoid transformation, it appears unrealistic that half of the compounds are missing at lower temperatures (especially in the light of large number of samples claimed to be prepared). Consequently, both works can hardly be considered complete and refer to outdated/incomplete results, and the phase equilibria there must be revisited, if not reinvestigated from scratch. In this work, we report the synthesis and structural characterization of four new ternary silicides: $LaNi_5Si_2$, $La_2Ni_8Si_3$, $LaNi_5Si_3$ and $La_3Ni_4Si_2$.

EXPERIMENTAL SECTION

Synthesis. All alloys were prepared starting from the same pure elements: La pieces (99.9 wt %), Ni slugs (99.99 wt %) and Si grains (99.999 wt %). Samples with different compositions ($La_{9.5}Ni_{57.2}Si_{33.3}$, $La_{17.8}Ni_{54.6}Si_{27.6}$, $La_{33.34}Ni_{44.44}Si_{22.22}$, $La_{12.5}Ni_{58.75}Si_{28.75}$) and a total mass of about 1 g each were arc melted in high-purity argon atmosphere using Ti ingot as a getter. The buttons were remelted at least twice after turning them upside-down to ensure good homogenization. Weight losses after arc melting never exceeded 0.5

Received: August 21, 2024
Revised: October 21, 2024
Accepted: November 7, 2024
Published: November 18, 2024

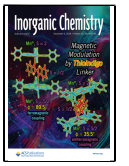

ACS Publications
© 2024 The Authors. Published by American Chemical Society

https://doi.org/10.1021/acs.inorgchem.4c03560
Inorg. Chem. 2024, 63, 22761−22770

Table 1. Overview of Representative Compounds Featuring a Metal Lonsdaleite Framework

	M/Ae[a]	space group	ST	a (Å)	b (Å)	c (Å)	β (deg)	refs
$BaAg_{4.9}Al_{2.1}$	7	$P\bar{6}2m$	own	8.913		7.278		41
$SrAu_4Ga_3$	7	$P\bar{6}2m$	$BaAg_{4.9}Al_{2.1}$	8.609		7.204		42
$SrAu_5Al_2$	7	$Pnma$	own	8.942	7.232	9.918		43
$BaAu_5Ga_2$	7	$Pnma$	own	8.855	7.188	20.37		44
$LaNi_5Si_2$	7	$Pnma$	$BaAu_5Ga_2$	7.8223(7)	6.3894(6)	17.843(2)		
$Ba_{1.04}Au_{4.5}Ga_{2.4}$	6.6	$P\bar{6}2m$	own	8.789		7.212		44
$Eu_{1.1}Au_{4.4}Ga_{2.2}$	6	$P\bar{6}2m$	own	8.543		7.249		44
$Ae_2Au_6T_3$	4.5	$R\bar{3}c$	own	∼8.72		∼21.3		45−49
Ae = Sr, Ba, or Eu; T = Zn, Cd, Al, Ga, In, or Sn								
$Sr_2Au_7T_2$	4.5	$C2/c$	own	∼15.0	∼8.56	∼8.67	∼124	43, 45
T = Zn, Al, or Ga								
$Ca_4Au_{10}Zn_3$	3.25	$C2/c$	own	15.98	8.197	11.88	120.9	50
$Cu_{2.88}As$	–	$\overline{P3}c1$	own	7.110		21.879		51

[a]M/Ae = anion/cation ratio.

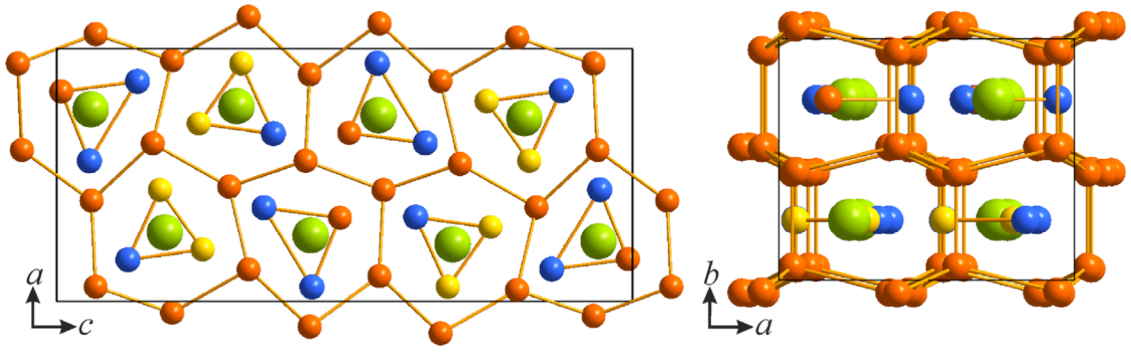

Figure 1. Projections of the crystal structure of $LaNi_5Si_2$ along the b (left) and c (right) crystallographic axes. Honeycombs are alternatively filled with La or Ni/Si triangles. La atoms are colored green, Ni atoms orange, Si atoms blue, and mixed Ni/Si positions yellow.

wt %. After melting, the as-cast samples were placed in Ta foil, closed in evacuated fused silica tubes and annealed at 1273 K for 7−14 days. The $La_3Ni_4Si_2$ sample was annealed at 873 K for 1 month. At the end of the heat treatment, samples were cooled to room temperature by switching off the furnace. Single crystals of the new ternary compound were isolated from the crushed samples. The samples were stable in air for at least months in any form.

Single-Crystal and Powder X-ray Diffraction. Powder patterns were collected using a Panalytical powder diffractometer (Bragg−Brentano geometry, Ni-filtered Cu Kα radiation) in the 10−90° 2ϑ range, with 0.02° 2ϑ step and counting times of 15−20 s per step. Phase analyses were performed using the WinXPow 3.1 program (STOE & Cie GmbH). The FullProf program package was applied for Rietveld analysis of the collected data sets.[21] Selected powder pattern Rietveld refinements have been provided in Supporting Information revealing the complexity of the phase space with multiphase products (Figures S1−S4).

Single-crystal X-ray diffraction (XRD) measurements were performed at room temperature on a Bruker D8 Venture diffractometer operating at 50 kV and 1.4 mA equipped with a Photon 3 CMOS detector, a flat graphite monochromator, and a Mo Kα IμS 3.0 microfocus source (λ = 0.71073 Å). The raw frame data were collected and handled using the Bruker APEX3 software package (Bruker AXS, 2015). Absorption correction has been performed using the multiscan method (SADABS).[22,23] Initial models of the crystal structures were obtained with the program SHELXT-2014[24] and refined with SHELXL-2014[25] within the APEX3 software package. Anisotropic displacement parameters have been refined for all atoms. Reflection intensities and symmetries were carefully re-examined with the aid of the PLATON program to exclude any missing higher symmetry.[26−29] The program DIAMOND was used for drawing and analyzing the crystal structure.[30]

Electronic Structure Calculations. Tight binding electronic structure calculations for idealized $LaNi_5Si_2$ were performed according to the linear muffin-tin-orbital (LMTO) method in the atomic sphere approximation (ASA).[31,32] The problem of occupational disorder has been treated by assigning fully occupied Ni and Si positions, respectively, for both Ni/Si positions. The only drawback of this model is the appearance of short Si−Si bonds, which do not exist in the real structure and will be discussed separately (see below). The radii of the Wigner-Seitz spheres were assigned automatically to guarantee the best match between the overlapping and full potentials.[33] They were determined to be 2.22 and 2.06 Å for La, 1.33, 1.31, 1.36, 1.31, 1.32, and 1.30 Å for Ni and 1.37, 1.39, 1.38, and 1.38 Å for Si. No empty spheres were needed to fully occupy the space. The basis sets were 6s/(6p)/5d/4f for La, 4s/4p/3d for Ni and 3s/3p/(3d) for Si with orbitals in parentheses downfolded.[34] The convergence criterion was set to 10^{-5} eV. The band structure was sampled for 196 k-points in the irreducible wedges of the Brillouin zone. Crystal orbital Hamilton populations (COHPs) as well as their weighted sums (ICOHPs)[35] have been calculated and analyzed to provide insights into the bonding situations in the crystal structure.

RESULTS AND DISCUSSION

Our previous screening of the La−Ni−Si system revealed that, despite intensive explorations, such systems may still contain unexplored or overlooked areas with plenty of unknown compounds.[16,17] Indeed, research in similar systems has intensified recently confirming our expectations. For instance, the isothermal section of the Ce−Ni−Si system was constructed just in 2016,[36] however, a very fresh investigation from 2024 (just a few months ago), revealed additional compounds following isocompositional findings in the La−

https://doi.org/10.1021/acs.inorgchem.4c03560
Inorg. Chem. 2024, 63, 22761−22770

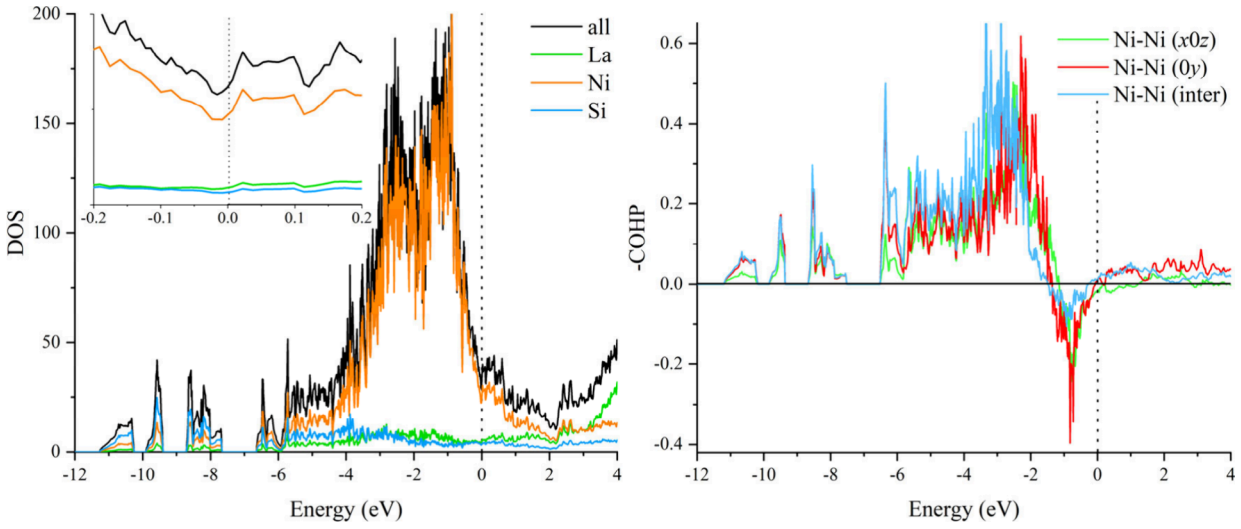

Figure 2. Density of states (left) and crystal orbital Hamilton populations (right) for $LaNi_5Si_2$. The Fermi levels are marked with dotted lines.

Ni−Si system.[37] Although obtained in the same system, some compounds have different stability ranges that may frequently not overlap.

$LaNi_5Si_2$ crystallizes in the orthorhombic space group *Pnma* (a = 7.8223(7), b = 6.3894(6), c = 17.843(2) Å, V = 891.8(2) Å^3, Z = 8) and belongs to the larger family of compounds formed by a combination of group II−III metal/transition metal/*p*-element and which is represented mostly with Au as the transition metal (see Table 1). A prominent feature of the family is the formation of a transition metal homoatomic framework with the structure of lonsdaleite, which is sometimes also addressed as hexagonal diamond.[38] It is interesting to note that such a framework has never been observed for any pure metal, while the reported structure of lonsdaleite itself is still under discussion and may not exist independently.[39,40] A quick inspection of the phase space around the discovered compositions showed the existence of isostructural $CeNi_{4.95}Si_{2.05(1)}$ (a = 7.774(2), b = 6.390(2), c = 17.539(5) Å, V = 871.2(4) Å^3), while homologous honeycomb compounds specifically in the La−Ni−Si system are not excluded although have not yet been confirmed.

As $LaNi_5Si_2$ is isostructural to $BaAu_5Ga_2$,[44] it will primarily be compared to the latter. In $LaNi_5Si_2$, the diamond-type network is formed of Ni atoms, while the honeycomb cavities are filled with single La atoms or $NiSi_2$ triangles (Figure 1). Although the compound appears to be a Daltonide, a significant amount of occupational disorder involving two Ni/Si positions is observed. These positions show preferred occupation by Ni and Si, respectively, while the ratio is well counterbalanced practically approaching stoichiometric composition. Identical behavior was observed in the prototype compound as well. In $LaNi_5Si_2$, there are two types of Ni/Si triangles; those involving disordered Ni/Si sites are more regular (d_{Ni-Ni} and d_{Ni-Si} are in the range 2.283−2.397(6) Å), while those with fully occupied pure Ni and Si positions are significantly elongated showing visible separation of the Si vertices (d_{Ni-Si} = 2.333−2.385(6) Å and d_{Si-Si} = 2.889(7) Å). This distortion is more substantial than in the parent Au compound and may be due to competing strong Ni−Si interactions within the triangles and between them and the framework. Ni/Si triangles and La alternate within the framework honeycombs.

It is worth noting that the formation of the diamond framework was attributed to the relativistic effects of Au and to the presence of corresponding strong Au−Au interactions helping to stabilize the construct.[43] That consideration was in line with the experimental discoveries that all observed compounds featuring a lonsdaleite substructure were observed for Au compounds, with just one Ag representative as an exclusion (Table 1). Although Au and Ag bear many similarities, their intermetallic structural chemistry usually shows substantial differences, particularly in complex intermetallics.[52] In this light, the observation of another isostructural compound with Ni is astonishing, although corresponding 2D honeycomb constructs with Ni are known.[53,54] As a separate branch, we shall also mention the LaF_3 structure type[55] where lonsdaleite motifs are formed with uniform filling of the honeycombs although without dominating homoatomic bonding. In this context, the Cu_3M (M = P, As) binaries[51] which crystallize with the anti-LaF_3 type of structure are interesting as they offer additional possibilities for discovery of lonsdaleite frameworks with other transition metals. In this respect, we analyzed geometric and electronic patterns throughout the entire series.

From the geometric point of view, it sounds logical that smaller La (covalent radius = 2.07 Å) forms the structure with smaller Ni and Si (1.24 and 1.11 Å),[14] while bulkier Ba (2.15 Å) was observed with bigger Au and Ga (1.36 and 1.22 Å). Unfortunately, we cannot extend this analysis for the entire series as structural distortions affect geometric criteria, and no other Ni/Si structures have been detected yet. For instance, the smallest Ca (1.76 Å) forms a singularity in the family, belonging to a monoclinic structure with no reported isostructural compounds yet,[50] while the biggest Ag (1.45 Å) is known only in combination with the biggest Ba (2.15 Å).[41] Even the isocompositional compound $SrAu_5Al_2$ with the slightly smaller Sr (1.95 Å) revealed some geometric changes (Table 1) to stabilize the lonsdaleite framework. Although it is rather hard to predict new element combinations, more extensive synthetic explorations may help to complement the database of lonsdaleite frameworks in intermetallics and perform a comprehensive analysis.

From the electronic side, since the framework is formed of electron-poorer Ni, both the cation (La) and the *p* element

https://doi.org/10.1021/acs.inorgchem.4c03560
Inorg. Chem. 2024, 63, 22761−22770

Table 2. Bond Lengths, −ICOHP Values, and Bonding Contributions in $LaNi_5Si_2$

bond type	length (Å)	−ICOHP (eV/average bond)	no. per cell	−ICOHP (eV/cell)	contribution (%)
Ni−Ni (0*y*)	2.496−2.593	0.97	16	15.5	3.8
Ni−Ni (*x*0*z*)	2.583−2.805	0.85	40	34.1	8.3
Ni−Ni (inter)	2.432−2.522	1.29	48	61.8	15.1
					27.2
Ni−Si (triangular)	2.272−2.375	2.02	28	56.6	13.8
Ni−Si (inter)	2.301−2.497	1.88	92	174	42.4
					56.2
La−Ni	2.918−3.443	0.34	120	41.3	10.1
La−Si	3.168−3.611	0.28	56	15.8	3.8
Si−Si	2.385−2.878	1.35	8	10.7	2.6
La−La	4.412−4.497	0.06	8	0.45	0.1

(Si) are electron-richer, pointing to an electronic origin of the structure stabilization. In fact, Au compounds are electron-richer having *vec* (valence electron count) 13 for the isocompositional compounds ($BaAu_5Ga_2$ and $SrAu_5Al_2$) compared to 11 in $LaNi_5Si_2$. To further elucidate this aspect, we continued with the inspection of the electronic structure and bonding picture along the series.

The electronic density of states (DOS) is characterized by broad overlaps across the entire energy range and a small local minimum at the Fermi energy, E_F, being typical for intermetallic compounds (Figure 2 and S5). The area between −6 and +1 eV is dominated by Ni-*d* states. La-*f* states can be observed at energies ≥3 eV. A distinct pseudogap could only be observed at around 2 eV above the Fermi level and can only serve as an indication of the preference of the structure type to accommodate more electrons following the experimental observations. On the other hand, Ni-*d* states are located directly at the Fermi level pointing toward the possibility of their inclusion in the *vec* schemes to compensate for the electron deficiency. The band structure of $LaNi_5Si_2$ (Figure S6) indicates some electronic instability at the Fermi level, particularly around Y and G points, that may be due to possible magnetic ordering of Ni atoms or superconductivity. Performing a spin-polarized calculation for deeper analysis is difficult because of the structural complexity. However, it has to be noted that, Ni mostly does not order magnetically in similar compounds.[56] Superconductivity has though been observed at 1.8 K in another disordered La−Ni silicide $La_5Ni_{1.75}Si_3$.[57]

A comprehensive analysis of the bonding in $LaNi_5Si_2$ has been performed using the crystal orbital Hamilton populations COHP scheme with particular focus on bonding patterns within the homoatomic Ni diamond framework, see Figure 2. While the Ni−Ni interactions are all bonding up to about −1 eV, they turn strongly antibonding at this point up to the Fermi level. Such a situation has been observed in intermetallics for other homoatomic transition metal interactions, like Au, Pd or Pt and is commonly associated with d^{10}-d^{10} repulsion.[58−64] A subtle difference can be observed in the Ni−Ni interactions along different crystallographic directions. Ni−Ni interactions in the six-membered Ni rings with boat-conformation running parallel to the *b* axis, normal to the $NiSi_2$ triangular plane, are bonding at E_F and stay bonding well above it. The same was observed for the Ni−Ni interactions between the lonsdaleite framework and the $NiSi_2$ triangles, while Ni−Ni contacts within the condensed network of six-membered Ni rings with chair-conformation in the *ac* plane are antibonding up to 1 eV above the Fermi level. A similar bonding behavior has also been observed in the gold prototype.[44] However, relativistic effects of gold may play a significant role in softening those antibonding interactions allowing for a large diversity of the homoatomic motifs.[65] Thus, homoatomic transition metal framework is not stable on its own, justifying its nonexistence with pure metals, but needs supporting interactions for stabilization.

It is not unexpected that heteroatomic Ni−Si bonds provide the largest contribution to the total bonding (Table 2 and S10), particularly those between the triangles and the Ni framework. Although numerous, the contributions from the Ni−Ni pairs are significantly smaller yet comparable to Au−Au's contribution in the related Au lonsdaleite structures.[46] Interestingly, the number and contributions from the framework Ni−Ni pairs and supporting Ni−Ni interactions involving $NiSi_2$ triangles are practically identical. Populations involving the formal cation La, result in 14% of the total. This number is high with respect to alkali and alkaline-earth interactions,[44,66] but indicates a somewhat lower involvement of La in the bonding with Ni compared to heavier transition metals.[58,63] Somewhat higher numbers for the Si−Si interactions are due to the model used for the calculation and, in part, represent Ni−Si interactions. True Si−Si (2.878 Å) as well as La−La contacts represent a negligible component of the interactions in $LaNi_5Si_2$.

$La_2Ni_8Si_3$ crystallizes in the tetragonal space group $P4_2/nmc$ (a = 10.0278(3), c = 7.5047(4) Å, V = 754.65(6) Å^3, Z = 4) and crystallizes with the $Eu_2Ni_8Si_3$ type[67] and its antitype analogue $Sr_2Pt_3Al_8$.[68] The crystal structure can be described based on two sets of tetrahedral motifs alternating along three crystallographic axes. In the first one, La_4 tetrahedra alternate along the *c* axis with Ni_4 tetrahedra, each surrounded by a Si_4 square (Figure 3). The second set is purely anionic and consists of edge-sharing $SiNi_4$ tetrahedra surrounded by Ni_4 rectangles. The connectivity between both sets is established solely via Ni−Si contacts between the Si_4 squares and the Ni_4 rectangles surrounding the inner tetrahedra.

The coordination environment of two Ni positions is trigonal antiprismatic ($Ni@Ni_6$) with a different degree of capping. One of them is capped equatorially by two Si and three La atoms, while the other is by a Si_4 tetrahedron and three additional La atom. The last Ni is coordinated by five Ni, three Si and three La positions in the form of a distorted tricapped (Ni+Si+La) tetragonal prism ($Ni@Ni_4Si_2La_2$). Si coordination environments are best described as tetracapped (2 Ni + 2 La) $Si@Ni_6$ trigonal prism and a slightly distorted Frank-Kasper polyhedron with CN = 12 (8 Ni + 4 La). Due to the segregation of the La atoms forming tetrahedra, the

https://doi.org/10.1021/acs.inorgchem.4c03560
Inorg. Chem. 2024, 63, 22761−22770

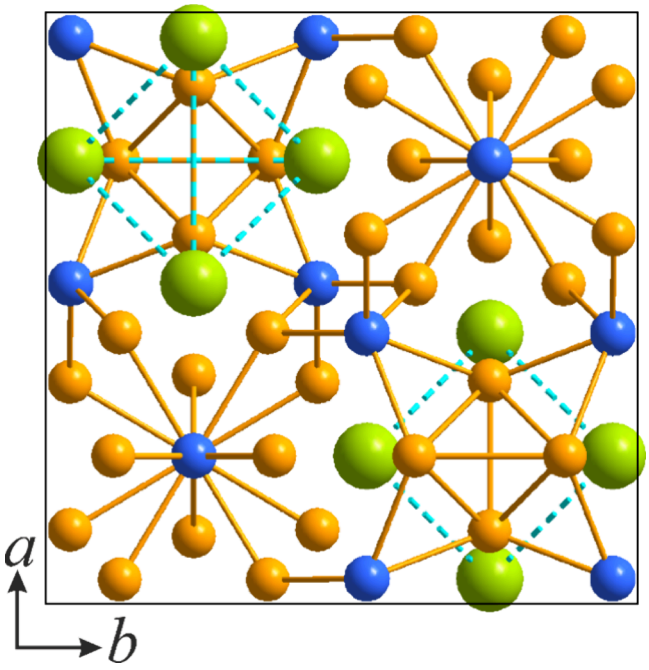

Figure 3. Projection of the crystal structure of $La_2Ni_8Si_3$ along the crystallographic *c* axis. La atoms are colored green, Ni atoms orange, and Si atoms blue.

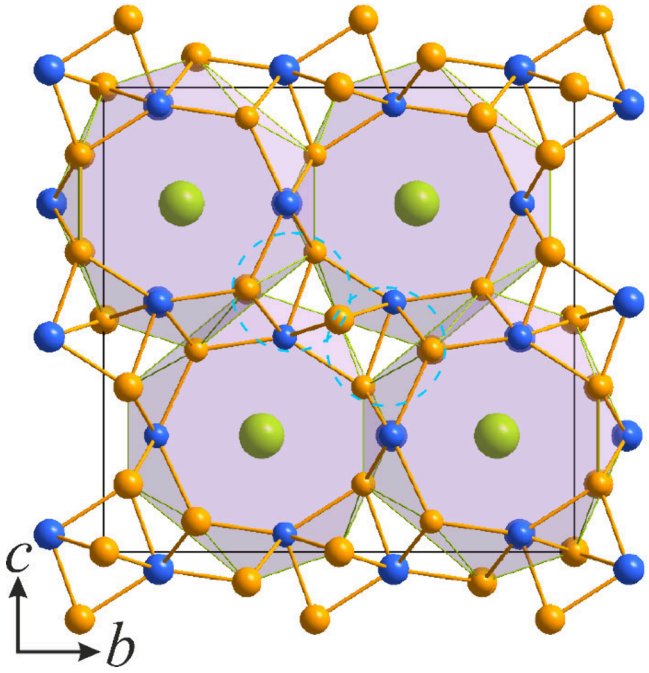

Figure 4. Projection of the crystal structure of $LaNi_5Si_3$ on the *bc* plane. La atoms are colored green, Ni atoms orange, and Si atoms blue.

coordination environment of the latter is highly irregular having CN = 17 ($La@Ni_9Si_5La_3$). It is interesting to note that despite higher symmetry the distribution of the Ni−Si and Ni−Ni distances is quite broad -2.272−2.608(2) and 2.393−2.731(1) Å. Both lower edges of the ranges start slightly below the sum of the corresponding covalent radii. Similarly to $La_3Ni_4Si_2$, no Si−Si bonds could be observed here. Not surprisingly (as the compositions are just 3 at. % away from each other) the entire bonding spectrum is equally represented by the cation−anion (La−Ni(Si)) contacts − 72 + 40, Ni−Ni − 88, and Ni−Si bonds − 92 showing very close proportions to $LaNi_5Si_2$ (see Table S7) and correspondingly similar ICOHP contributions (Table S11).

$LaNi_5Si_3$ crystallizes in the orthorhombic space group *Cmcm* (*a* = 3.722(2), *b* = 11.759(5), *c* = 11.622(3) Å, *V* = 508.7(3) Å^3, Z = 4) and belongs to the $SrNi_5P_3$ structure type being the first silicide representative of the latter. Practically all compounds crystallizing in that type have also been reported with Ni and large formal cations, i.e. Sr, Eu and La[69−72] suggesting the high importance of the geometric factor for this type of structure.

The crystal structure of $LaNi_5Si_3$ consists of a set of straight tunnels extending along the *a* axis (Figure 4). The tunnels are formed by stacking $La@Ni_{14}Si_7$ polyhedra with two large open faces. Such polyhedra consist of three parallel planar 7−7−7 membered rings. It is worth noting that despite the high diversity this population of rings has not been observed in the intermetallics with larger Au.[65] The neighboring tunnels share common triangular faces but such stacking leads to solely anionic chains between each three of them in the form of stacking edge-sharing tetrahedra. The latter form dumbbells via common vertices (Figure 4, dashed circles).

All Ni positions in the structure exhibit a distorted equatorially tetracapped tetragonal prismatic or highly distorted icosahedral environment (CN = 12) − $Ni@Ni_7Si_2La_3$, $Ni@Ni_5Si_4La_3$ and $Ni@Ni_6Si_4La_2$. Si positions have coordination numbers 9 and tricapped trigonal prismatic coordination − $Si@Ni_6La_3$ and $Si@Ni_7La_2$. All polyhedra for this and the following structures have been illustrated in Figure S7. Ni−Si and Ni−Ni contacts in the structure are in relatively narrow ranges of 2.2331−2.4045(9) and 2.4291−2.7160(7) Å. Practically all Ni−Si contacts are below the sum of the corresponding covalent radii suggesting strong interactions. Interestingly, Si−Si contacts of 2.865(1) Å are present being comparable to those found in $LaNi_5Si_2$. Of course, such distance is far away from any bonding interaction highlighting the tendency of Si atoms to avoid any direct interaction. A somewhat higher Si proportion in the formula unit is reflected in the number of Ni−Si contacts in the structure −68 as compared to Ni−Ni−48 or La−Ni + La−Si−40 + 28, respectively (Table S8). This points to optimization of the heteroatomic bonding in contrast to Ni−Ni clustering in two previous structures.

$La_3Ni_4Si_2$ was not detected in the samples that were annealed at 1270 or even 1070 K while good quality crystals were observed after slow cooling and prolonged annealing at 870 K. This compound crystallizes in the $Ce_3Ni_4Si_2$ type of structure[37] (SG *C*2/*c*, *a* = 15.819(1), *b* = 6.0068(5), *c* = 7.4918(6) Å, *β* = 103.163(5)°, *V* = 693.17(10) Å^3, *Z* = 4). Its crystal structure is best represented in terms of polyanionic framework with encapsulated formal cations, *i.e.* La atoms (Figure 5). Ni and Si atoms form tunnels along the *c* axis, while La atoms are arranged in zigzag chains inside. From this point of view, the structure is quite uniform although the Ni/Si ratio may vary within the tunnels around two different La sites. Due to the higher electronegativity of La, it is less of an electron donor in contrast to alkali metal and participates more significantly in covalent bonding. Therefore, the polyanionic tunnel structure contains more open faces in contrast to similar compounds with active metals, *e.g.* AAu_3Ga_2 (*A* = K−Cs).[59,60]

Alternatively, the crystal structure of $La_3Ni_4Si_2$ can be presented in terms of layered packing and is a part of the

https://doi.org/10.1021/acs.inorgchem.4c03560
Inorg. Chem. 2024, 63, 22761−22770

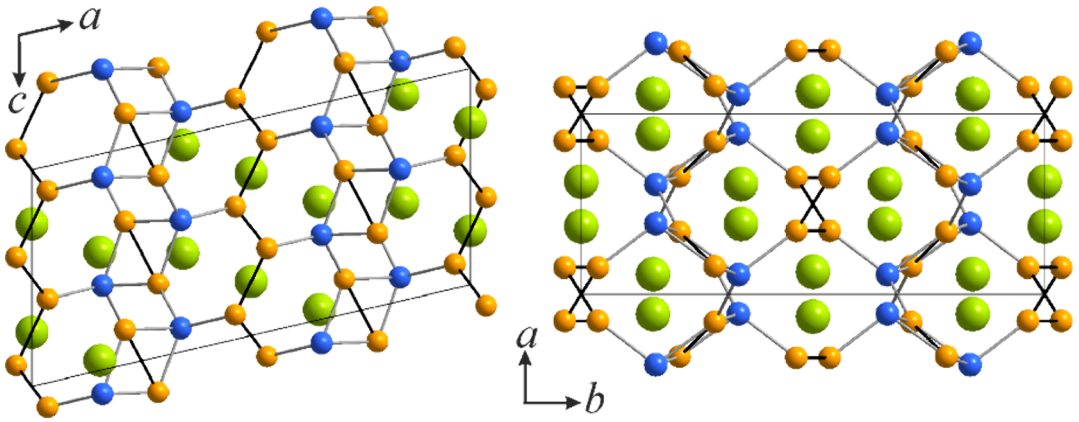

Figure 5. Projection of the crystal structure of $La_3Ni_4Si_2$ on the *ac* and *ab* planes, respectively. La atoms are colored green, Ni atoms orange, and Si atoms blue.

compositional sequence with a fixed La/Si ratio and close structural relationships. It is also worth noting that such sequences are rather common in the La−Ni−Si system with already reported two homologous series. This particular sequence here comprises $La_3Ni_3Si_2$[17] ($Ce_3Rh_3Si_2$ structure type),[73] $La_3Ni_{3.5}Si_2$[17] ($Pr_6Ni_7Si_4$ structure type)[74] and the newly uncovered $La_3Ni_4Si_2$. Each of these structures consists of a set of alternating slabs, namely LaNiSi (A), LaNi (B) and $LaNi_2$ (C) (Figure 6). The compositionally intermediate $La_3Ni_{3.5}Si_2$ exhibits structural features of both $La_3Ni_3Si_2$ and $La_3Ni_4Si_2$. Slab A is the most complex being represented by a nearly planar rhombi-octagonal tiling. Such motifs of a different degree of corrugation are rather common in polar intermetallics, particularly with late transition metals.[75,76] In the crystal structure of $La_3Ni_4Si_2$, slabs C are represented by Ni dumbbell zigzag chains serving as connectors between the neighboring slabs A, slightly shifted along the *c* axis. Interestingly, interslab connectivity is established solely via Ni−Si contacts.

The coordination environment of the La positions is quite irregular due to large open faces with coordination numbers ranging from 12 to 13. La1 is surrounded by eight Ni, four Si and an additional La atoms, while La2 is coordinated to eight Ni and 4 Si. With some degree of approximation, the latter polyhedron can be described as an irregular equatorially bicapped pentagonal prism. Additionally, there are five and eight La atoms in their second coordination spheres, respectively, centering large, open faces. All Ni and Si positions are surrounded by capped trigonal La_6 prisms. Both Ni positions are capped equatorially only with three (2Ni + Si) or four (Ni + 3Si) atoms, while the $SiLa_6$ polyhedron is tricapped equatorially and monocapped axially solely by Ni atoms. Ni−Si and Ni−Ni contacts in the structure are concentrated in narrow ranges of 2.352−2.459(1) Å and 2.572−2.665(1) Å, respectively, at or slightly above the sum of the corresponding covalent radii.[14] No Si−Si bonds could be observed in the structure.

As this composition stays away from three previous structures, it makes more sense to compare it to the other member of the homologous series we analyzed in our previous work. The total bonding spectrum is visibly dominated by the cation−anion contacts −106 + 46, while Ni−Ni bonding is practically absent−only 12 contacts and Ni−Si bonds are maximized −72 (Table S9). This picture is practically identical to two other members of the series, i.e. $La_3Ni_3Si_2$ and

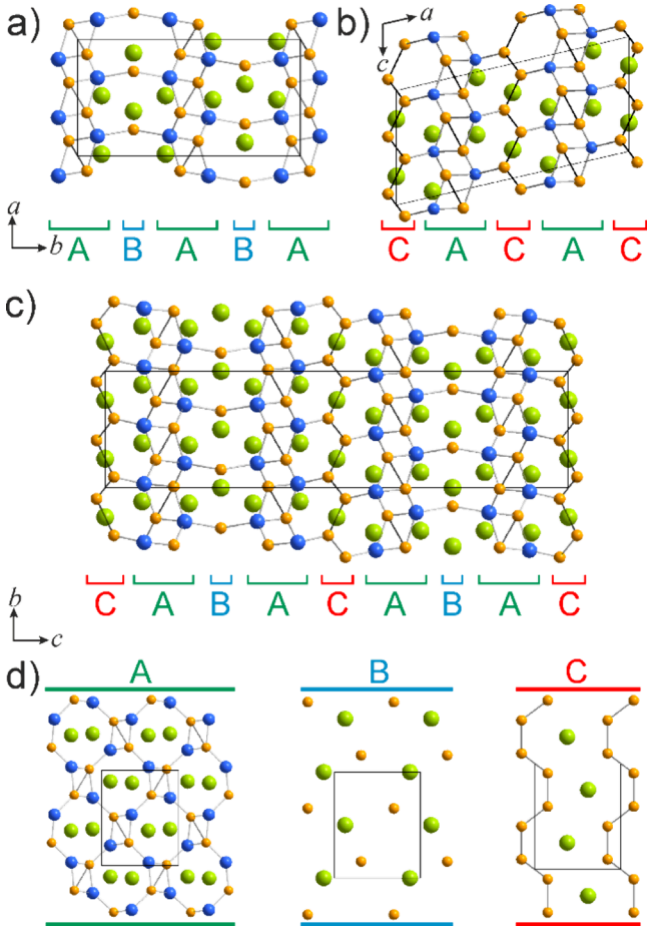

Figure 6. Comparison of the crystal structures of (a) $La_3Ni_3Si_2$, (b) $La_3Ni_4Si_2$, and (c) $La_3Ni_{3.5}Si_2$ and (d) projections of the constituent slabs extending normal to the projection planes. La atoms are colored green, Ni atoms orange, and Si atoms blue.

$La_3Ni_{3.5}Si_2$ as well as two other compositionally close compounds $LaNi_2Si$ and $La_2Ni_3Si_2$.[17] Of no surprise anymore, being not the major component quantitatively the heteroatomic Ni−Si contacts always provide the largest contributions to the total bonding. These contributions are comparable to the as a rule less represented homoatomic Ni−Ni bonds, while the cation−anion pairs contributions are minimal at the single

https://doi.org/10.1021/acs.inorgchem.4c03560
Inorg. Chem. 2024, 63, 22761−22770

bond level but statistically the most represented and therefore significant (15−30% of the total ICOHP).

Note. At the time of submission, we were made aware of another recently published manuscript that reports the structural properties of $La_3Ni_4Si_2$ from powder data and provides a different perspective of this homologous series.[37]

CONCLUSIONS

The La−Ni−Si system appears to be a gold mine for compounds of compositional and structural diversity. The system was intensively explored with the first reports starting in 1965[77] and the first attempt to construct an isothermal section at 670 K appeared 20 years later.[78] Due to the enormous complexity, limitations of the available methods at that time and noncoordinated efforts later, the full picture of the system has not emerged until now. The recent known attempts to construct similar isothermal sections for the La−Ni−Si system at different temperatures cannot be considered reliable due to the significant number of missing known ternaries.[19,20] The most recent attempt of a systematic phase space exploration in similar systems was carried out for Ce−Ni−Si, Gd−Ni−Si and Dy−Ni−Si in 2014−2016 reporting 26 and 20 and 21 compounds, respectively[36,79,80] showing a noticeable difference between the light and heavy lanthanide systems. Despite numerous representations, the following research brought three more new compounds in Ce−Ni−Si,[37] however, even more compounds exist there as was shown in this work.

Active exploration of the La−Ni−Si system are still ongoing. For instance, the area around "$LaNi_6Si_6$" has been examined together with isocompositional Ce−Ni−Si compounds,[36] while the Si-poorer part in the middle of the system was explored in our previous work leading to eight new compounds within two homologous series.[16,17] Certain experimental challenges are coming from significantly variable existence ranges for some compositionally close compounds. For example, $La_3Ni_4Si_2$, in contrast to all other members of its homologous series, could not easily be detected at 1070 or even 970 K, while growing single crystals at 870 K required slow cooling and prolonged annealing. Shifting the exploration toward the Ni-richer areas revealed four more compounds, namely $La_2Ni_8Si_3$, $LaNi_5Si_2$, $LaNi_5Si_3$ and $La_3Ni_4Si_2$. $LaNi_5Si_2$ is the first Ni representative of a larger family typically formed by aurides, $La_3Ni_4Si_2$ is a part of a local homologous series, while two remaining compounds bear some close analogies with phosphides or platinides. This brings the total number of discovered compounds to 33 as of now (Figure 7) and the ternary system in general as being one of the most populated, i.e. a gold mine of intermetallics. Taking into account the data from the closely related systems, even more compounds can be expected at least in the Ni-rich corner and still have to be discovered.

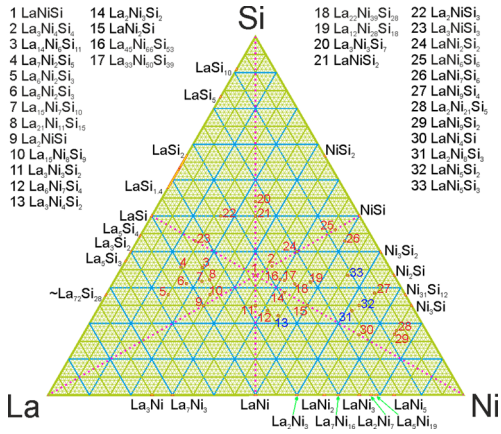

Figure 7. Map of the previously reported (marked with red numbers) and newly discovered (blue) La−Ni silicides.

ASSOCIATED CONTENT

Supporting Information

The Supporting Information is available free of charge at https://pubs.acs.org/doi/10.1021/acs.inorgchem.4c03560.

Rietveld refinements and additional details of the electronic structure calculations, Figures S1−S6, and Tables S1−S11 (PDF)

Accession Codes

Deposition Numbers 2375099−2375103 contain the supplementary crystallographic data for this paper. These data can be obtained free of charge via the joint Cambridge Crystallographic Data Centre (CCDC) and Fachinformationszentrum Karlsruhe Access Structures service.

AUTHOR INFORMATION

Corresponding Authors

Marcella Pani − *DCCI, Department of Chemistry and Industrial Chemistry, University of Genova, Genova 16146, Italy; Institute SPIN-CNR, Genova 16452, Italy;* Email: marcella.pani@unige.it

Pietro Manfrinetti − *DCCI, Department of Chemistry and Industrial Chemistry, University of Genova, Genova 16146, Italy; Institute SPIN-CNR, Genova 16452, Italy;* Email: pietro.manfrinetti@unige.it

Anja-Verena Mudring − *intelligent Advanced Materials, Department of Biological and Chemical Engineering and iNANO, Aarhus University, 8000 Aarhus C, Denmark; Department of Materials and Environmental Chemistry, Stockholm University, Stockholm 10691, Sweden; Department of Physics, Umeå University, 901 87 Umeå, Sweden;* orcid.org/0000-0002-2800-1684; Email: anja-verena.mudring@bce.au.dk, anja-verena.mudring@umu.se

Authors

Volodymyr Smetana − *intelligent Advanced Materials, Department of Biological and Chemical Engineering and iNANO, Aarhus University, 8000 Aarhus C, Denmark; Department of Materials and Environmental Chemistry, Stockholm University, Stockholm 10691, Sweden;* orcid.org/0000-0003-0763-1457

Davide Grilli − *Department of Materials and Environmental Chemistry, Stockholm University, Stockholm 10691, Sweden; DCCI, Department of Chemistry and Industrial Chemistry, University of Genova, Genova 16146, Italy; Institute SPIN-CNR, Genova 16452, Italy*

Vitalii Shtender − *Department of Chemistry - Ångström Laboratory, Uppsala University, Uppsala 75121, Sweden;* orcid.org/0000-0002-8690-9957

Complete contact information is available at: https://pubs.acs.org/10.1021/acs.inorgchem.4c03560

https://doi.org/10.1021/acs.inorgchem.4c03560
Inorg. Chem. 2024, 63, 22761−22770

Author Contributions

D.G. and V. Shtender: methodology and experiments. D.G. and V. Smetana: analysis, visualization, and writing of the manuscript. D.G., V. Smetana, and V. Shtender: analysis. A.-V.M., P.M., and M.P.: conceptualization, resources, supervision, writing, and review and editing. All of the authors participated in reviewing the entire manuscript.

Notes

The authors declare no competing financial interest.

■ ACKNOWLEDGMENTS

D.G. thanks the Erasmus+ program of the European Union for financial support. The research was supported by the Swedish Energy Agency (Energimyndigheten) through Grant 48699-1 (NNF SMARTER).

■ REFERENCES

(1) Kumar, K. S. Intermetallics: Silicides. In *Encyclopedia of Materials: Metals and Alloys*; Caballero, F. G., Ed.; Elsevier, 2001; pp 335−338.
(2) Schlesinger, M. E. Thermodynamics of solid transition-metal silicides. *Chem. Rev.* **1990**, *90* (4), 607−628.
(3) Villars, P.; Cenzual, K. Pearson's Crystal Data - Crystal Structure Database for Inorganic Compounds, Release 2021/22; ASM International: Materials Park, OH, 2022.
(4) Fitzer, E.; Mäurer, H. J.; Nowak, W.; Schlichting, J. Aluminium and silicon base coatings for high temperature alloys—Process development and comparison of properties. *Thin Solid Films* **1979**, *64* (2), 305−319.
(5) C Patnaik, P. Intermetallic coatings for high temperature applications-a review. *Material and manufacturing process* **1989**, *4* (1), 133−152.
(6) Chen, L. J. Metal silicides: An integral part of microelectronics. *JOM* **2005**, *57* (9), 24−30.
(7) Zhang, S.-L.; Östling, M. Metal Silicides in CMOS Technology: Past, Present, and Future Trends. *Crit. Rev. Solid State Mater. Sci.* **2003**, *28* (1), 1−129.
(8) Chen, X.; Liang, C. Transition metal silicides: fundamentals, preparation and catalytic applications. *Catal. Sci. Technol.* **2019**, *9* (18), 4785−4820.
(9) Pecharsky, A. O.; Gschneidner, K. A.; Pecharsky, V. K. The giant magnetocaloric effect of optimally prepared $Gd_5Si_2Ge_2$. *J. Appl. Phys.* **2003**, *93* (8), 4722−4728.
(10) Liu, X. B.; Altounian, Z.; Tu, G. H. The structure and large magnetocaloric effect in rapidly quenched LaFe11.4Si1.6 compound. *J. Phys.-Condens. Matter* **2004**, *16* (45), 8043.
(11) Lee, W. H.; Yang, F. A.; Shih, C. R.; Yang, H. D. Crystal structure and superconductivity in the Ni-based ternary compound LaNiSi. *Phys. Rev. B* **1994**, *50* (9), 6523−6525.
(12) Braun, H. F. Superconductivity of rare earth-iron silicides. *Phys. Lett. A* **1980**, *75* (5), 386−388.
(13) Morozkin, A. V.; Klyamkin, S. N.; Verbetsky, V. N.; Lushnikov, S. N.; Portnoy, V. K.; Movlaev, E. A.; Chernavskii, A. P.; Tarasov, A. V. Hydrogen sorption in homologous lanthanum and cerium nickel silicides. *J. Alloys Compd.* **2000**, *309* (1), 197−200.
(14) Cordero, B.; Gomez, V.; Platero-Prats, A. E.; Reves, M.; Echeverria, J.; Cremades, E.; Barragan, F.; Alvarez, S. Covalent radii revisited. *Dalton Trans.* **2008**, No. 21, 2832−2838.
(15) Allred, A. L. Electronegativity values from thermochemical data. *J. Inorg. Nucl. Chem.* **1961**, *17* (3), 215−221.
(16) Grilli, D.; Smetana, V.; Ahmed, S. J.; Shtender, V.; Pani, M.; Manfrinetti, P.; Mudring, A.-V. $La_{n(n+1)+x}Ni_{n(n+5)+y}Si_{(n+1)(n+2)-z}$: A Symmetric Mirror Homologous Series in the La-Ni-Si System. *Inorg. Chem.* **2023**, *62* (27), 10736−10742.
(17) Pani, M.; Provino, A.; Smetana, V.; Shtender, V.; Bernini, C.; Mudring, A. V.; Manfrinetti, P. Four Ternary Silicides in the La-Ni-Si System: From Polyanionic Layers to Frameworks. *CrystEngComm* **2022**, *24*, 8219−8228.
(18) Prots, Y. M.; Jeitschko, W. Lanthanum Nickel Silicides with the General Formula $La_{(n+1)(n+2)}Ni_{n(n-1)+2}Si_{n(n+1)}$ and Other Series of Hexagonal Structures with Metal:Metalloid Ratios Close to 2:1. *Inorg. Chem.* **1998**, *37* (21), 5431−5438.
(19) Zhang, T.; Wang, K.; Huang, K.; Yao, Q.; Lu, Z.; Long, Q.-X.; Deng, J.; Wang, J.; Zhou, H. Experimental Investigation of Isothermal Section in the La-Ni-Si System at 1073 K. *SSRN* **2024**, DOI: 10.2139/ssrn.4760404.
(20) Zhou, H.; Yao, Q.; Yuan, S.; Liu, J.; Deng, H. Phase relationships in the La-Ni-Si system at 673 K. *J. Alloys Compd.* **2004**, *366* (1), 161−164.
(21) Rodríguez-Carvajal, J. Recent developments of the program FULLPROF, in commission on powder diffraction (IUCr). *Newsletter* **2001**, *26*, 12−19.
(22) Blessing, R. H. An empirical correction for absorption anisotropy. *Acta Crystallogr., Sect. A* **1995**, *51* (1), 33−38.
(23) Krause, L.; Herbst-Irmer, R.; Stalke, D. An empirical correction for the influence of low-energy contamination. *J. Appl. Crystallogr.* **2015**, *48* (6), 1907−1913.
(24) Sheldrick, G. SHELXT - Integrated space-group and crystal-structure determination. *Acta Crystallogr., Sect. A* **2015**, *71* (1), 3−8.
(25) Sheldrick, G. Crystal structure refinement with SHELXL. *Acta Crystallogr. Sect. C: Struct. Chem.* **2015**, *71* (1), 3−8.
(26) Spek, A. Single-crystal structure validation with the program PLATON. *J. Appl. Crystallogr.* **2003**, *36* (1), 7−13.
(27) Spek, A. Structure validation in chemical crystallography. *Acta Crystallogr. Sect. D* **2009**, *65* (2), 148−155.
(28) Spek, A. L. What makes a crystal structure report valid? *Inorg. Chim. Acta* **2018**, *470*, 232−237.
(29) Spek, A. checkCIF validation ALERTS: what they mean and how to respond. *Acta Crystallogr. E* **2020**, *76* (1), 1−11.
(30) *DIAMOND: Program for Crystal and Molecular Structure Visualization*; Crystal Impact GbR: Bonn, Germany, 2011.
(31) *TB-LMTO-ASA*; Max-Planck-Institut für Festkörperforschung: Stuttgart, Germany, 1994.
(32) Andersen, O. K.; Jepsen, O. Explicit, First-Principles Tight-Binding Theory. *Phys. Rev. Lett.* **1984**, *53* (27), 2571−2574.
(33) Jepsen, O.; Andersen, O. K. Calculated electronic structure of the sandwichd1 metals LaI_2 and CeI_2: Application of new LMTO techniques. *Z. Phys. B. Cond. Mater.* **1995**, *97* (1), 35−47.
(34) Lambrecht, W. R. L.; Andersen, O. K. Minimal basis sets in the linear muffin-tin orbital method: Application to the diamond-structure crystals C, Si, and Ge. *Phys. Rev. B* **1986**, *34* (4), 2439−2449.
(35) Dronskowski, R.; Bloechl, P. E. Crystal orbital Hamilton populations (COHP): energy-resolved visualization of chemical bonding in solids based on density-functional calculations. *J. Phys. Chem.* **1993**, *97* (33), 8617−8624.
(36) Morozkin, A. V.; Knotko, A. V.; Garshev, A. V.; Yapaskurt, V. O.; Nirmala, R.; Quezado, S.; Malik, S. K. The Ce-Ni-Si system as a representative of the rare earth-Ni-Si family: Isothermal section and new rare-earth nickel silicides. *J. Solid State Chem.* **2016**, *243*, 290−303.
(37) Failamani, F.; Grytsiv, A.; Bursik, J.; Giester, G.; Rogl, P. The Ce-Ni-Si System Revisited: More Homologue Compounds? *Inorg. Chem.* **2024**, *63* (19), 8604−8614.
(38) Frondel, C.; Marvin, U. B. Lonsdaleite, a Hexagonal Polymorph of Diamond. *Nature* **1967**, *214* (5088), 587−589.
(39) Németh, P.; Garvie, L. A. J.; Aoki, T.; Dubrovinskaia, N.; Dubrovinsky, L.; Buseck, P. R. Lonsdaleite is faulted and twinned cubic diamond and does not exist as a discrete material. *Nat. Commun.* **2014**, *5* (1), 5447.
(40) McCulloch, D. G.; Wong, S.; Shiell, T. B.; Haberl, B.; Cook, B. A.; Huang, X.; Boehler, R.; McKenzie, D. R.; Bradby, J. E. Investigation of Room Temperature Formation of the Ultra-Hard Nanocarbons Diamond and Lonsdaleite. *Small* **2020**, *16* (50), 2004695.

(41) Cordier, G.; Röhr, C. Zur kenntnis der ternären aluminide $Ba_5Cu_{1,9}Al_{3,1}$, $BaAg_{2,4}Al_{2,6}$, $Ba_{16}Ag_7Al_{27}$ und $Ba_3Ag_{14,6}Al_{6,4}$. *J. Less Common Met.* **1991**, *170* (2), 333−357.
(42) Seidel, S.; Hoffmann, R.-D.; Pöttgen, R. $SrAu_4Ga_3$: a further example with Ga_3 units and a Lonsdaleite-related gold substructure. *Monatsh. Chem.* **2014**, *145* (7), 1043−1049.
(43) Palasyuk, A.; Grin, Y.; Miller, G. J. Turning Gold into "Diamond": A Family of Hexagonal Diamond-Type Au-Frameworks Interconnected by Triangular Clusters in the Sr-Al-Au System. *J. Am. Chem. Soc.* **2014**, *136* (8), 3108−3117.
(44) Smetana, V.; Steinberg, S.; Card, N.; Mudring, A.-V.; Miller, G. J. Crystal Structure and Bonding in $BaAu_5Ga_2$ and $AeAu_{4+x}Ga_{3-x}$ (Ae = Ba and Eu): Hexagonal Diamond-Type Au Frameworks and Remarkable Cation/Anion Partitioning in the Ae-Au-Ga Systems. *Inorg. Chem.* **2015**, *54* (3), 1010−1018.
(45) Mishra, T.; Lin, Q.; Corbett, J. D. Gold Network Structures in Rhombohedral and Monoclinic $Sr_2Au_6(Au,T)_3$ (T = Zn, Ga). A Transition via Relaxation. *Inorg. Chem.* **2013**, *52* (23), 13623−13630.
(46) Lin, Q.; Mishra, T.; Corbett, J. D. Hexagonal-Diamond-like Gold Lattices, Ba and $(Au,T)_3$ Interstitials, and Delocalized Bonding in a Family of Intermetallic Phases $Ba_2Au_6(Au,T)_3$ (T = Zn, Cd, Ga, In, or Sn). *J. Am. Chem. Soc.* **2013**, *135* (30), 11023−11031.
(47) Gerke, B.; Hoffmann, R.-D.; Pöttgen, R. Zn_3 and Ga_3 Triangles as Building Units in $Sr_2Au_6Zn_3$ and $Sr_2Au_6Ga_3$. *Z. Anorg. Allg. Chem.* **2013**, *639* (14), 2444−2449.
(48) Gerke, B.; Pöttgen, R. $Sr_2Au_6Al_3$ and $Eu_2Au_6Al_3$ - First Representatives of the $Sr_2Au_6Zn_3$ Type with Aluminum Triangles. *Z. Naturforsch., B* **2014**, *69* (1), 121−124.
(49) Gerke, B.; Korthaus, A.; Niehaus, O.; Haarmann, F.; Pöttgen, R. Triangular Zn_3 and Ga_3 units in $Sr_2Au_6Zn_3$, $Eu_2Au_6Zn_3$, $Sr_2Au_6Ga_3$, and $Eu_2Au_6Ga_3$ - structure, magnetism, ^{151}Eu Mössbauer and $^{69;71}$Ga solid state NMR spectroscopy. *Z. Naturforsch., B* **2016**, *71* (5), 567−577.
(50) Gerke, B.; Hoffmann, R.-D.; Pöttgen, R. $Ca_4Au_{10}Zn_3$ - A Substitution Variant of AlB_2 by Incorporation of Zn_3 Triangles. *Z. Anorg. Allg. Chem.* **2015**, *641* (12−13), 2174−2180.
(51) Mödlinger, M.; Provino, A.; Solokha, P.; Caglieris, F.; Ceccardi, M.; Macciò, D.; Pani, M.; Bernini, C.; Cavallo, D.; Ciccioli, A.; et al. Cu_3As: Uncommon Crystallographic Features, Low-Temperature Phase Transitions, Thermodynamic and Physical Properties. In *Materials*; 2023; Vol. *16*.
(52) Bigun, I.; Steinberg, S.; Smetana, V.; Mudryk, Y.; Kalychak, Y.; Havela, L.; Pecharsky, V.; Mudring, A.-V. Magnetocaloric Behavior in Ternary Europium Indides EuT_3In: Probing the Design Capability of First-Principles-Based Methods on the Multifaceted Magnetic Materials. *Chem. Mater.* **2017**, *29* (6), 2599−2614.
(53) Shtender, V.; Smetana, V.; Crivello, J. C.; Gondek, L.; Przewoźik, J.; Mudring, A. V.; Sahlberg, M. Honeycomb Constructs in the La-Ni Intermetallics: Controlling Dimensionality via Element Substitution. *Inorg. Chem.* **2023**, *62* (37), 14843−14851.
(54) Shtender, V.; Smetana, V.; Crivello, J.-C.; Kravets, A.; Gondek, Ł.; Mudring, A.-V.; Sahlberg, M. Intermetallics of 4:4:1 and 3:3:1 series in La-(Co,Ni)-M (M = Bi, Pb, Te, Sb, Sn and Ga, Al) systems and their properties. *J. Alloys Compd.* **2024**, *982*, 173767.
(55) Gregson, D.; Catlow, C. R. A.; Chadwick, A. V.; Lander, G. H.; Cormack, A. N.; Fender, B. E. F. The structure of LaF_3 - a single-crystal neutron diffraction study at room temperature. *Acta Crystallogr. Sect. B* **1983**, *39* (6), 687−691.
(56) Belkhiria, S.; Briki, C.; Dhaou, M.; Alresheedi, F.; Jemni, A. A study of the magnetic properties of $LaNi_5$ and their effect on hydrogen desorption under the action of a magnetostatic field. *Heliyon* **2023**, *9* (10), No. E20311.
(57) Lee, B. K.; Ryu, D. H.; Kim, D. Y.; Hong, J. B.; Jung, M. H.; Kitazawa, H.; Suzuki, O.; Kimura, S.; Kwon, Y. S. Magnetic ordering in frustrated $Ce_5Ni_2Si_3$. *Phys. Rev. B* **2004**, *70* (22), 224409.
(58) Provino, A.; Steinberg, S.; Smetana, V.; Paramanik, U.; Manfrinetti, P.; Dhar, S. K.; Mudring, A.-V. Gold in the layered structures of $R_3Au_7Sn_3$: from relativity to versatility. *Cryst. Growth Des.* **2016**, *16* (10), 5657−5668.
(59) Smetana, V.; Corbett, J. D.; Miller, G. J. Four polyanionic compounds in the K-Au-Ga system: a case study in exploratory synthesis and of the art of structural analysis. *Inorg. Chem.* **2012**, *51* (3), 1695−1702.
(60) Smetana, V.; Miller, G. J.; Corbett, J. D. Three Alkali-Metal-Gold-Gallium Systems. Ternary Tunnel Structures and Some Problems with Poorly Ordered Cations. *Inorg. Chem.* **2012**, *51* (14), 7711−7721.
(61) Provino, A.; Steinberg, S.; Smetana, V.; Kulkarni, R.; Dhar, S. K.; Manfrinetti, P.; Mudring, A.-V. Gold-rich $R_3Au_7Sn_3$: establishing the interdependence between electronic features and physical properties. *J. Mater. Chem. C* **2015**, *3* (32), 8311−8321.
(62) Samal, S. L.; Gulo, F.; Corbett, J. D. Cluster Chemistry in Electron-Poor Ae-Pt-Cd Systems (Ae = Ca, Sr, Ba): $(Sr,Ba)Pt_2Cd_4$, $Ca_6Pt_8Cd_{16}$, and Its Known Antitype $Er_6Pd_{16}Sb_8$. *Inorg. Chem.* **2013**, *52* (5), 2697−2704.
(63) Samal, S. L.; Corbett, J. D. Synthesis, structure, and bonding analysis of the polar Intermetallic phase Ca_2Pt_2Cd. *Z. Anorg. Allg. Chem.* **2012**, *638* (12−13), 1963−1969.
(64) Gui, X.; Sobczak, Z.; Klimczuk, T.; Xie, W. Pt-rich intermetallic APt_8P_2 (A = Ca and La). *J. Alloys Compd.* **2019**, *798*, 53−58.
(65) Smetana, V.; Rhodehouse, M.; Meyer, G.; Mudring, A.-V. Gold polar intermetallics: structural versatility through exclusive bonding motifs. *Acc. Chem. Res.* **2017**, *50* (11), 2633−2641.
(66) Smetana, V.; Lin, Q.; Pratt, D. K.; Kreyssig, A.; Ramazanoglu, M.; Corbett, J. D.; Goldman, A. I.; Miller, G. J. A Sodium-Containing Quasicrystal: Using Gold To Enhance Sodium's Covalency in Intermetallic Compounds. *Angew. Chem., Int. Ed.* **2012**, *51* (51), 12699−12702.
(67) Belan, B.; Bel'skii, V.; Pecharskii, V.; Bodak, O.; Zhuk, T. Crystal structure of europium nickel silicide ($Eu_2Ni_8Si_3$). *Dop. Akad. Nauk Ukrain RSR, Seriya A* **1986**, *48*, 63−65.
(68) Stegemann, F.; Block, T.; Klenner, S.; Zhang, Y.; Fokwa, B. P. T.; Doerenkamp, C.; Eckert, H.; Janka, O. Structural, Physical, Theoretical and Spectroscopic Investigations of Mixed-Valent $Eu_2Ni_8Si_3$ and Its Structural Anti-Type $Sr_2Pt_3Al_8$. *Eur. J. Inorg. Chem.* **2021**, *2021* (37), 3832−3845.
(69) Probst, H.; Mewis, A. Ternäre Nickelphosphide und -arsenide mit einem Metall: Nichtmetall-Verhältnis von 2:1. *Z. Anorg. Allg. Chem.* **1991**, *597* (1), 173−182.
(70) Badding, J. V.; Stacy, A. M. Synthesis and crystal structure of a new europium nickel phosphide phase, $EuNi_5P_3$. *J. Solid State Chem.* **1987**, *67* (2), 354−358.
(71) Davydov, V.; Kuz'ma, Y. B. Crystal structure of lanthanum cobalt phosphide $LaCo_5P_3$. *Dop. Akad. Nauk Ukrain RSR, Seriya A* **1981**, *43*, 81−84.
(72) Hofmann, W. K.; Jeitschko, W. Structural investigations of ternary lanthanoid and uranium nickel phosphides. *J. Solid State Chem.* **1984**, *51* (2), 152−158.
(73) Prots, Y. M.; Stęień-Damm, J.; Salamakha, P. S.; Bodak, O. I. The crystal structure of orthorhombic $Ce_3Rh_3Si_2$, an intergrowth of FeB- and YPd_2Si-type slabs. *J. Alloys Compd.* **1997**, *256* (1), 166−169.
(74) Hovestreydt, E.; Parthe, E. Hexapraseodymium heptanickel tetrasilicide, $Pr_6Ni_7Si_4$, an intergrowth of $ThSi_2$- and $Y_3Rh_2Si_2$-type slabs. *Acta Crystallogr. C* **1984**, *40* (12), 1992−1995.
(75) Li, B.; Corbett, J. D. Different Cation Arrangements in Au-In Networks. Syntheses and Structures of Six Intermetallic Compounds in Alkali-Metal-Au-In Systems. *Inorg. Chem.* **2007**, *46* (15), 6022−6028.
(76) Thronberens, W.; Sinnen, H.-D.; Schuster, H.-U. Ternäre phasen der alkalimetalle mit palladium beziehungsweise platin und silizium, germanium beziehungsweise zinn mit kanal-strukturen. *J. Less Common Met.* **1980**, *76* (1), 99−108.
(77) Gladyshevskii, E.; Bodak, O. Compounds with Structures of the AlB_2 Type in the System Ce-Ni-Si and in Related Systems. *Dopov. Akad. Nauk Ukr. RSR* **1965**, 601−604.
(78) Bodak, O. I.; Gladyshevskii, E. I. *Troinye sistemy soderzhashchie redkozemelnye metally: spravochnik (in russian)*; Shkola, V., Ed.; Lviv Univesrity: Lviv, Ukraine, 1985.

https://doi.org/10.1021/acs.inorgchem.4c03560
Inorg. Chem. 2024, 63, 22761−22770

(79) Morozkin, A. V.; Knotko, A. V.; Yapaskurt, V. O.; Manfrinetti, P.; Pani, M.; Provino, A.; Nirmala, R.; Quezado, S.; Malik, S. K. The isothermal section of Gd-Ni-Si system at 1070K. *J. Solid State Chem.* **2016**, *235*, 58−67.
(80) Yuan, F.; Mozharivskyj, Y.; Morozkin, A. V.; Knotko, A. V.; Yapaskurt, V. O.; Pani, M.; Provino, A.; Manfrinetti, P. The Dy-Ni-Si system as a representative of the rare earth-Ni-Si family: Its isothermal section and new rare-earth nickel silicides. *J. Solid State Chem.* **2014**, *219*, 247−258.

https://doi.org/10.1021/acs.inorgchem.4c03560
Inorg. Chem. 2024, 63, 22761−22770